University of Nebraska at Omaha
DigitalCommons@UNO

Mathematics Faculty Publications | Department of Mathematics

6-2007

The Stabilizing Effect of Noise on the Dynamics of a Boolean Network

Christopher S. Goodrich
University of Nebraska at Omaha, cgoodrich@unomaha.edu

Mihaela Teodora Matache
University of Nebraska at Omaha, dvelcsov@unomaha.edu

Follow this and additional works at: https://digitalcommons.unomaha.edu/mathfacpub

 Part of the Mathematics Commons

Recommended Citation

Goodrich, Christopher S. and Matache, Mihaela Teodora, "The Stabilizing Effect of Noise on the Dynamics of a Boolean Network" (2007). *Mathematics Faculty Publications*. 21.
https://digitalcommons.unomaha.edu/mathfacpub/21

This Article is brought to you for free and open access by the Department of Mathematics at DigitalCommons@UNO. It has been accepted for inclusion in Mathematics Faculty Publications by an authorized administrator of DigitalCommons@UNO. For more information, please contact unodigitalcommons@unomaha.edu.

THE STABILIZING EFFECT OF NOISE ON THE DYNAMICS OF A BOOLEAN NETWORK

CHRISTOPHER S. GOODRICH, MIHAELA T. MATACHE*

Department of Mathematics, University of Nebraska at Omaha, Omaha, NE 68182-0243, USA

*Phone: 402-554-3295, Fax: 402-554-2975, dmatache@mail.unomaha.edu

Abstract. In this paper, we explore both numerically and analytically the robustness of a synchronous Boolean network governed by rule 126 of cellular automata. In particular, we explore whether or not the introduction of noise into the system has any discernable effect on the evolution of the system. This noise is introduced by changing the states of a given number of nodes in the system according to certain rules. New mathematical models are developed for this purpose. We use MATLAB to run the numerical simulations including iterations of the real system and the model, computation of Lyapunov exponents, and generation of bifurcation diagrams. We provide a more in-depth fixed-point analysis through analytic computations paired with a focus on bifurcations and delay plots to identify the possible attractors. We show that it is possible either to attenuate or to suppress entirely chaos through the introduction of noise and that the perturbed system may exhibit very different long-term behavior than that of the unperturbed system.

PACS: 05.45.-a; 02.70.-c; 87.10.+e; 89.75.-k

Keywords: synchronous Boolean network, robustness, noise, ECA rule 126, system dynamics, stability

1. Introduction

In the past few years, there has been rather intense study regarding cellular automata and Boolean networks, their association, and their applications to various applied problems in the physical, biological, chemical, and social sciences, as well as neural, artificial, and complex networks in general (e.g. [1] - [15]).

A cellular automaton refers to a dynamical system of nodes which is discrete in space and time, and operates on a uniform, regular lattice [16]. The network is characterized by local interactions between the nodes, so that the state of a node at time $t + 1$ is determined by the states at time t of a finite number of nodes in the network (called its neighborhood of parents).

Typically, the nodes are updated synchronously. The impact of topological and dynamic noise on complex patterns of cellular automata has been recently studied by Marr and Hütt in [17].

A Boolean network is similar and, in fact, strongly related to the cellular automata. In particular, in a Boolean network there exists, again, a set of nodes operating on each other according to a predetermined rule. However, in the case of a Boolean network, there does not exist a particular spatial structure that is induced by the nodes. Also, it is not required that the update rule be uniform, whereas this a requirement in cellular automata – that is, in a Boolean network, it may be the case that the update rule varies from one node to another. At the same time, the network can evolve asynchronously. The interest for Boolean networks has increased since the publication of Kauffman's "Origins of order" [18], whose work on the self-organization and adaptation in complex systems has inspired many other research studies.

Now, there are myriad Boolean rules that one may employ in cellular automata and Boolean networks. One of the most well studied of these is the so-called Rule 126. This particular rule asserts, in summary, that a cell dies only if there is overcrowding or not enough support, and has been studied extensively by Matache et.al. [12]- [15], by Andrecut and Ali [2], [19]. Rule 126 can be described as

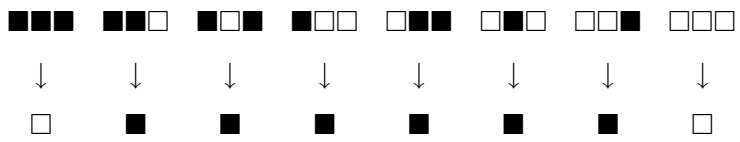

where black is ON and white is OFF. As explained in [13], rule 126 is one of several which exhibit randomly distributed triangular shapes of arbitrarily large size. This makes rule 126 a class III of complexity generating rule [16]. Rule 126 is useful as a conceptual model of (biological) cell growth and of a (chemical) catalytic process because the central site survives (or is born) unless the neighborhood is too poorly populated or too crowded, in which case it dies. It is interesting that Rule 126 is both a very simple growth model and yet exhibits a quite sophisticated dynamic behavior. In Figure 1 we provide pattern formation graphs for an elementary cellular automaton with 200 nodes (horizontally) and 200 steps of evolution of the network (downward) after a transient period of 400 time steps. The top graph is for an unperturbed network, while the bottom graph is for the same network in which, at each time step, a random selection of 5% of the nodes switch their values (and thus do not follow Rule 126). We can see how the patterns change after the induction of noise in the system.

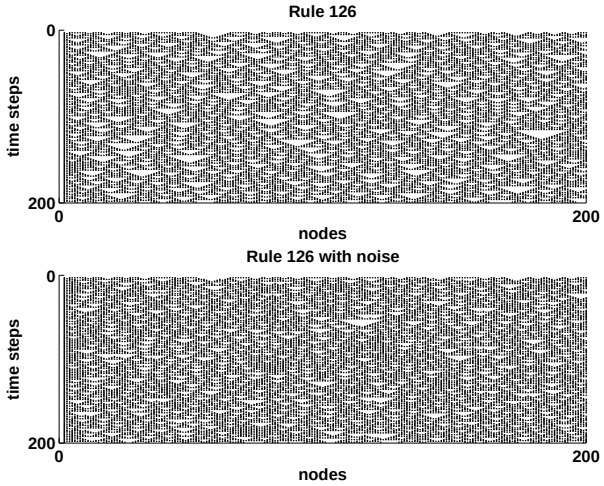

FIGURE 1. ECA with 200 nodes and 200 time steps of evolution. The top graph represents an unperturbed network governed by rule 126. The bottom graph represents a network under the same rule, perturbed by noise: at each time step, 5% of the nodes switch their values artificially. We observe the changes induced by the noise.

The studies mentioned above identify the dynamics of Boolean networks governed by rule 126 under various assumptions: fixed or variable number of parents, synchronous or asynchronous updating of the nodes involving a variety of updating schemes, deterministic or stochastic. Thus the robustness of these models with respect to randomness in the updates or asynchronism has been studied. It has been observed that a large connectivity is in general associated with order in the system, and that for a small connectivity the system may exhibit order or chaos. When a small number of nodes is updated at the same time, the system is mainly ordered. However, none of the studies mentioned above discusses the robustness to perturbations generated by intrinsic changes in the state of the nodes (e.g. gene regulation). It is known that real networks (biological/genetic, physical, neural, chemical, social etc.) are always subject to disturbances and have the ability to reach functional diversity and aim to maintain the same state under environmental noise (e.g. food source or energy changes). There are intrinsic or environmental disturbances as well as possible mutations within the network (e.g. genetic mutations). Inducing disturbance in the system by changing the value of certain nodes in the network (according to a deterministic or stochastic rule) is a good model for an environmental or intrinsic type of perturbation. A similar procedure has been used for example by Bilke and Sjunnesson [20] where one randomly chosen variable is inverted after the system has reached a limit cycle in the Kauffman model. In this paper we study the robustness of a synchronous Boolean network

governed by rule 126 of cellular automata under perturbations induced by changing in two different ways (to be explained) the state of randomly selected nodes at each time point of the evolution of the system.

The robustness of Boolean models and cellular automata to asynchronism has also been studied by Chaves et.al. [3], [21], and by Fatès and Morvan [22]. Kauffman et.al. [10] and Shmulevich et.al. [23], [24] have been interested in random genetic models with canalyzing functions and Post classes which induce stability in the network and show robustness to perturbations. It has also been shown by Aldana and Cluzel [1] that the dynamical robustness of intracellular networks against variations of their internal parameters is a direct consequence of their scale-free topology. The dynamical organization in the presence of noise of a Boolean neural network with random connections has been analyzed by Huepe and Aldana-González in [9], showing that there is a critical value of the noise below which the network remains organized and above which it behaves randomly. Recently, Gershenson et.al. [25] showed that the addition of redundant nodes to random Boolean networks increases their robustness. The robustness to random and specific removal of vertices of a synchronization-preferential model of complex dynamical networks has been investigated by Fan et.al. in [26], showing that this model is more robust in comparison to the BA scale-free model [27] and the synchronization-optimal network model [28]. At the same time, Moreira et.al. [29] have applied noise to small-world networks to investigate a density-classification task as a model system for coordination and information processing in descentralized systems modeled as Boolean networks. They showed that simple heuristics such as a majority rule are efficient in noisy environments. Amaral et.al. [30] have shown that under the assumptions of a small-world topology and the presence of noise, the networks can generate complex behavior that can range from white-noise dynamics to long-range dependence and Brownian noise.

Thus the study of the robustness of a Boolean network to various types of perturbations is an important aspect of the evolution of systems under Boolean models. These systems have to respond and adapt to interior and exterior disturbances. Generally the interest is in suppressing chaos and bringing the system into an ordered regime. We will show in this paper that for the network under consideration, the introduction of noise can stabilize the system for a wide range of parameters.

In Section 2 of the paper we develop a mathematical model for a Boolean network that is subject to predetermined perturbation schemes. We study two noise models that reflect mostly

environmental or intrinsic types of perturbations that can affect a network. The models with attendant perturbation schemes, as we shall see, are capable of affecting multiple nodes at one, thus testing thoroughly the robustness of the proposed models. The models are as follows. The "flip" rule selects randomly j out of N nodes at each time point t and flips their values from 0 to 1 or viceversa, whichever the case may be. If $p(t)$ is the probability of finding a node in state 1 at time t and k is the fixed number of parents of each node, then it is shown that

$$p(t+1) = 1 - \left(p(t) + \frac{j}{N}(1-2p(t))\right)^{k+1} - \left(1 - p(t) - \frac{j}{N}(1-2p(t))\right)^{k+1}.$$

The second model, called the "0-1" rule, induces noise by randomly selecting j nodes at each time point t and changing their value to 1 with probability $\mathcal{P}$ and to 0 with probability $1-\mathcal{P}$. We show that in this case

$$p(t+1) = 1 - \left(p(t) + \frac{j}{N}(\mathcal{P} - p(t))\right)^{k+1} - \left(1 - p(t) - \frac{j}{N}(\mathcal{P} - p(t))\right)^{k+1}.$$

We study the robustness under the assumptions of both a fixed and a random parameter j.

A comparison of the noise models is provided in Section 3. The actual numerical testing of the robustness of the network is accomplished via Matlab and is presented in Section 4 of this paper, after which we look at a more analytical analysis of the robustness or lack thereof of our models in Section 5. Finally, in Section 6 we indicate some future directions that this work could take.

2. The Boolean Network Model

First, let us note that throughout the presentation that follows, we are using the description and notation of both [12] and [13]. These are made clear in the presentation below.

Now, consider a network with N nodes. Each node c_n, $n = 1, 2, \ldots, N$ can take on only two values 1 or 0. Often this is interpreted as a system in which each node can be either ON of OFF. At each time point t the system can be in one of the 2^N possible states. We assume that all the nodes update their value at the same time, that is the network is synchronous. The evolution of the nodes from time t to time $t+1$ is given by a Boolean rule which is considered the same for all nodes. Each node c_n is assigned a random "neighborhood" of parents, whose values at time t influence the value of c_n at time $t+1$ through the following Boolean rule. If $c_n(t)$ and all its parents have the same value at time t (that is they are all either 0 or 1), then $c_n(t+1) = 0$, otherwise $c_n(t+1) = 1$. The parents of a node are chosen randomly from the remaining $N-1$

nodes and do not change thereafter. More precisely, if a node has k parents, then a set of k nodes is chosen from the remaining $N-1$ nodes with probability $\frac{1}{\binom{N-1}{k}}$.

This model is a description of a random Boolean network for homogeneous Boolean functions. The system is described by the number of parents of each node. Observe that the quantity $N_1(t) := \sum_{n=1}^{N} c_n(t)$ gives the number of cells that are in state 1 at time t. The concentration of nodes in state 1 is given by $p(t) = \frac{1}{N}\sum_{n=1}^{N} c_n(t)$ and is used to estimate the probability of finding a node in state 1 at time t. In the paper [2] the authors show that $p(t+1)$ is given by

$$p(t+1) = 1 - p(t)^{k+1} - (1-p(t))^{k+1} \tag{1}$$

where $k \geq 1$ is the number of parents of each node (considered fixed in that paper).

Further extensions of this model have been provided in [12]- [15]. In particular, these studies conduct an extensive analysis of the cases in which either the number of parents of node may vary from node to node or the system itself is asynchronous, which is to say that not all nodes update at the same time.

To make this paper self-contained, we briefly recall the reasoning that leads to formula (1). Observe that $p(t+1) = \frac{1}{N}\left(N_{0\to 1}(t) + N_{1\to 1}(t)\right)$, where $N_{0\to 1}(t)$ represents the number of nodes that are 0 at time t and become 1 at time $t+1$, while $N_{1\to 1}(t)$ is the number of nodes that are 1 at time t and do not change their value at time $t+1$. But observe that a node can change from 0 to 1 if and only if at least one of its parents is 1 at time t by the Boolean rule 126. Thus $N_{0\to 1}(t) = N_0(t)\left(1-(1-p(t))^k\right)$ since $(1-p(t))^k$ is the probability that all the k parents are in state 0 at time t and therefore $1-(1-p(t))^k$ is the probability that at least one of the parents is 1. It is assumed that the parents act independently. Although in reality there are correlations between parent nodes, it has been shown in all the studies mentioned above [2], [12]- [15], that the models obtained through a mean-field approach are suitable for the real systems they model.

Similarly one obtains that $N_{1\to 1}(t) = N_1(t)(1-p(t)^k)$ since a node that is 1 at time t does not change its value if and only if at least one of its parents is 0 at time t. The probability of this event is $1-p(t)^k$. Replacing these formulae, one gets that $p(t+1) = \frac{N_0(t)}{N}(1-(1-p(t))^k) + \frac{N_1(t)}{N}(1-p(t)^k)$. But $\frac{N_1(t)}{N} = p(t)$ and $\frac{N_0(t)}{N} = 1-p(t)$ which leads to $p(t+1) = 1-(1-p(t))^{k+1} - p(t)^{k+1}$.

To study the robustness of the network to perturbations we first introduce noise in the system according to two schemes, called the "flip" rule and the "0-1" rule. The two schemes are as follows.

The system is iterated a number of times and thus allowed to reach a steady behavior (which could be ordered or not), say by time T. According to the "flip" rule, at each time point $t > T$ we randomly select j nodes of the network and flip their value (from 0 to 1 or from 1 to 0). According to the "0-1" rule, at each time point $t > T$ we randomly select j nodes of the network and change their values to 1 with probability $\mathcal{P}$ and to 0 with probability $1-\mathcal{P}$. We are interested in comparing the effects of the two types of noise, and in determining the magnitude of j that induces a qualitative change in the behavior of the system. Clearly $1 \leq j < N$.

Then we go one step further in the analysis, and we introduce more stochastic noise in the system by allowing the number j to vary at each time point according to a given random distribution or stochastic process. Again we wish to understand how robust is the system to these types of noise by varying the parameters of the distributions and random processes chosen.

We note here that the types of noise described above reflect mostly environmental or intrinsic types of disturbances that can affect say a biological or genetic network. For example, in [29] the authors apply a version of the "flip" rule in which the nodes switch their values with a given probability that parametrizes the intensity of the noise. A similar procedure is applied in [30]. On the other hand, genetic networks may exhibit genetic mutations which could be represented by addition or removal of nodes or connections in the network. The study of robustness to these other types of noise will make the object of future research.

We start with the "flip" rule which we describe in detail. We need to understand how the model (1) is changed under such a perturbation. Since the number of zeros and ones changes due to the perturbation, the value of $p(t)$ is modified prior to the application of the model (1). To determine the modified $p(t)$ we observe that if j nodes are chosen at random, then $j \cdot p(t)$ of them are in state 1 and $j \cdot (1 - p(t))$ are in state 0. By the flip rule, the total number of nodes in state 1 is decreased by $j \cdot p(t)$ since they are changed to 0. On the other hand the number is increased by $j \cdot (1 - p(t))$ since the zeros become ones. Thus, the proportion of nodes in state 1, that is $p(t)$, is modified as follows:

$$q(t) := p(t) - \frac{j \cdot p(t)}{N} + \frac{j \cdot (1 - p(t))}{N} = p(t) + \frac{j}{N}(1 - 2p(t)).$$

Observe that $q(t) \geq 0$ since all the terms are nonnegative in the above computation and since $j < N$. We also have that

$$q(t) \leq p(t) + (1 - 2p(t)) = 1 - p(t) \leq 1.$$

Thus $0 \leq q(t) \leq 1$.

For example, if $j = 1$, which means that we change only one node at a time, then

$$q(t) = p(t) + \frac{1}{N}(1 - 2p(t)) = \frac{1}{N} + \frac{N-2}{N}p(t). \tag{2}$$

We can summarize the above results in the following proposition.

Proposition 1. *Consider a Boolean network with N nodes as described above. If, beginning at time $T > 0$, we perturb the system at each time point $t > T$ by altering j nodes at a time according to the "flip" rule, then the probability that a node is ON (i.e., the node is in state 1) at time $t + 1$ is given by:*

$$p(t+1) = 1 - \left(p(t) + \frac{j}{N}(1 - 2p(t))\right)^{k+1} - \left(1 - p(t) - \frac{j}{N}(1 - 2p(t))\right)^{k+1}. \tag{3}$$

Proof. Immediate from the discussion above.

□

In a similar fashion we can determine a model for the perturbed system under the "0-1" rule. Again, to determine the modified $p(t)$ we observe that if j nodes are chosen at random, then $j \cdot p(t)$ of them are in state 1 and $j \cdot (1 - p(t))$ are in state 0. By the "0-1" rule, the total number of nodes in state 1 is decreased by $j \cdot p(t)$ and increased by $j \cdot \mathcal{P}$ since each selected node can become a 1 with probability $\mathcal{P}$. Thus, the proportion of nodes in state 1, that is $p(t)$, is modified as follows:

$$q(t) := p(t) - \frac{j \cdot p(t)}{N} + \frac{j \cdot \mathcal{P}}{N} = p(t) + \frac{j}{N}(\mathcal{P} - p(t)).$$

Observe that $q(t) \geq 0$ since all the terms are nonnegative in the above computation and $j < N$. We also have that

$$q(t) \leq p(t) + (\mathcal{P} - p(t)) = \mathcal{P} \leq 1.$$

Thus $0 \leq q(t) \leq 1$.

We give again the example for $j = 1$, which means that we change only one node at a time. Then

$$q(t) = p(t) + \frac{1}{N}(\mathcal{P} - p(t)) = \frac{\mathcal{P}}{N} + \frac{N-1}{N}p(t). \tag{4}$$

Thus the following proposition holds.

Proposition 2. *Consider a Boolean network with N nodes as described above. If, beginning at time $T > 0$, we perturb the system at each time point $t > T$ by altering j nodes at a time*

according to the "0-1" rule, then the probability that a node is ON (i.e., the node is in state 1*) at time* $t+1$ *is given by:*

$$p(t+1) = 1 - \left(p(t) + \frac{j}{N}(\mathcal{P} - p(t))\right)^{k+1} - \left(1 - p(t) - \frac{j}{N}(\mathcal{P} - p(t))\right)^{k+1}. \tag{5}$$

Now that we have the working models (3) and (5), we now are in a position to investigate numerically the robustness of the original system to the above perturbations. We do so in what follows. But first we provide a comparison of the two models to identify similarities and differences in the behavior of the noise.

We note that allowing j to be random does not change the actual models (3) and (5). The only difference is that in this case at each time point t, j will be the value of a random variable.

3. Comparison of Noise Rules

In this section we provide both a graphical and an analytical comparison of the two noise rules to understand how the parameters induce differences between the two models. We start this analysis by observing that the main terms generating differences between the formulas (3) and (5) are $j(1-2p(t))$ for the "flip" rule and $j(\mathcal{P}-p(t))$ for the "0-1" rule. To understand the differences or similarities between these two terms, we define the following functions:

$$f(p) = j_1(1-2p) \qquad \text{for the "flip" rule}$$

and

$$g(p) = j_2(\mathcal{P}-p) \qquad \text{for the "0-1" rule.}$$

We note that for $p \in [0,1]$ we have that $|f(p)| \leq j_1$ and $f(1/2) = 0$. For a fixed j_1 the graph is a line with negative slope equal to $-2j_1$ taking on a symmetric range of values from $-j_1$ to j_1. On the other hand, $-j_2(1-\mathcal{P}) \leq g(p) \leq j_2\mathcal{P}$ and $g(\mathcal{P}) = 0$. Thus small values of $\mathcal{P}$ give mostly negative values of $g(p)$ while large values of $\mathcal{P}$ yield mostly positive values of $g(p)$. The graph is again a line with slope $-j_2$. Observe that if $\mathcal{P} = 1/2$ then the second function can be written as

$$g(p) = \frac{j_2}{2}(1-2p)$$

and thus if $j_1 = \frac{j_2}{2}$ the two formulas are equivalent and the two rules generate the same behavior of the system. In conclusion, for $\mathcal{P} = 1/2$, the two noise rules can be made equivalent by doubling the number of nodes to be flipped by the "0-1" rule. However, for other values of $\mathcal{P}$ only the

concurrent impact of the j values and the p values would produce an equivalent behavior of the two models. Thus there is no unique combination of the parameters of the two models that can make them equivalent. They depend on the actual values of p. To understand even better this kind of relationship, we plot $f(p)$ and $g(p)$ versus p and j_2 for fixed values of j_1. In Figure 2 we set $j_1 = 30$ and $N = 128$ so that the allowable values of j_2 are $1, 2, \ldots, 127$. Here $\mathcal{P} = 1/2$. Observe that the values of $f(p)$ do not depend on j_2 so the graph we obtain is a plane with values of $f(p)$ between -30 and 30. The graph of $g(p)$ is superimposed as a surface that intersects the plane for $f(p)$ along $p = 1/2$ and along $j_2 = 60$. This corresponds exactly to our previous findings on the case $\mathcal{P} = 1/2$. Thus in this case there is a unique combination of values of $\mathcal{P}, j_1$, and j_2 that makes the two models equivalent. On the other hand, Figure 3 provides similar plots for the case $\mathcal{P} = 5/8$ with the other parameters fixed as before. We observe that the intersection of the surface $g(p)$ and of the plane $p(t)$ is a curve in the (p, j_2) plane that depends on both p and j_2. Actually there are two intersections, for values $p \in [0, 1/2]$ and for values $p \in [1/2, 1]$, both functions of p and j_2. Thus one cannot choose a combinations of parameters independent of p that would make the two formulas equivalent. In simulations we also observe a symmetric behavior as $\mathcal{P}$ increases in terms of ranges of values of p covered by the intersection, which shift from $[0, 1/2]$ to $[1/2, 1]$ with increased $\mathcal{P}$. At the same time, larger j_1 values are associated with a wider range of j_2 values for the intersection of the surfaces.

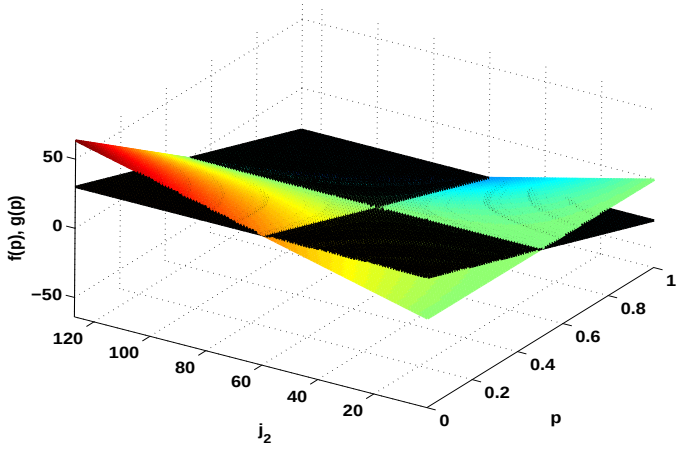

FIGURE 2. Plot of $f(p)$ and $g(p)$ versus $p \in [0, 1]$ and $j_2 \in \{1, 2, \ldots, 127\}$ for $j_1 = 30$ and $\mathcal{P} = 1/2$. The surface $g(p)$ intersects the plane $f(p)$ along the lines $p = 1/2$ and $j_2 = 60$.

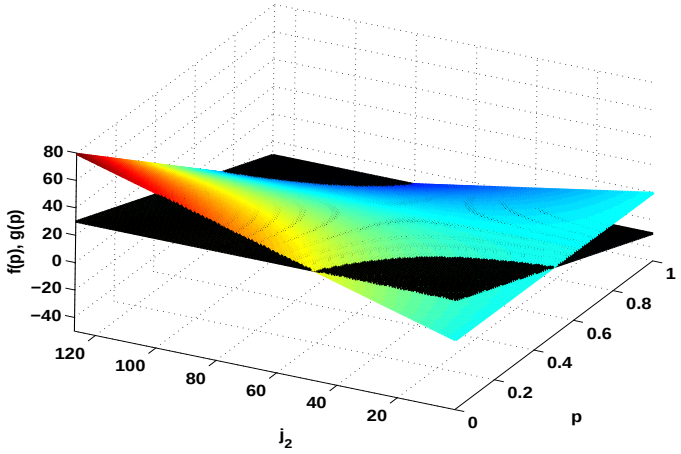

FIGURE 3. Plot of $f(p)$ and $g(p)$ versus $p \in [0,1]$ and $j_2 \in \{1,2,\ldots,127\}$ for $j_1 = 30$ and $\mathcal{P} = 5/8$. The surface $g(p)$ intersects the plane $f(p)$ along two curves for $p \in [0,1/2]$ and $p \in [1/2,1]$ respectively. We note that the intersection depends on both p and j_2.

We conclude that except for $\mathcal{P} = 1/2$, all other attempts to make the two functions $f(p)$ and $g(p)$ equivalent would have to take into account the current value of p, making the parameters functions of time.

Although the first iteration may not yield similar results with the two noise rules as explained above, we are interested in exploring the possibility that consecutive iterations of the models under the two rules may generate combinations of j_1 and j_2 that yield similar long term behavior of the two models regardless of the state of the system, that is the values of $p(t)$. To do this, we employ a simulation algorithm that iterates both models a number of times and identifies values of j_1 and j_2 that yield values $p(t)$ that are close for all possible ranges of initial conditions. More precisely, we select an initial value $p(0) \in [0,1]$ and generate its orbit under the "flip" rule (3), $\{p(0), p(1), \ldots, p(T)\}$ where $T = 50$ in the actual simulations. Using the same initial condition $q(0) = p(0)$ we construct its orbit under the "0-1" rule (5), $\{q(0), q(1), \ldots, q(T)\}$. We do this for many initial conditions that span the entire interval $[0,1]$. Let us denote the vector of initial conditions as follows $(p_1(0), p_2(0), \ldots, p_I(0))$ where $I \geq 100$ in the simulations. We compute the Euclidean distance between the vectors $(p_1(T), p_2(T), \ldots, p_I(T))$ and $(q_1(T), q_2(T), \ldots, q_I(T))$, namely $D(T) = \sqrt{\sum_{i=1}^{I} (p_i(T) - q_i(T))^2}$. We would like to identify pairs (j_1, j_2) that yield small differences $|p_i(T) - q_i(T)| \leq \epsilon$ for all $i = 1, 2, \ldots I$, where $\epsilon \in (0,1)$. In the simulations we use $\epsilon = 0.01$. Observe that if all the differences are this small then $D \leq \epsilon\sqrt{I}$. So for a given value of j_2 we search for the smallest value of j_1 for which $D \leq \epsilon\sqrt{I}$. Observe that although this

condition does not imply that all the distances are smaller than ϵ it insures that most of them are small enough, so that the two noise rules yield close values. Also, there might be larger values of j_1 for which D becomes even smaller. However, by choosing a small ϵ to begin with, we can make sure that the match is good anyway.

According to numerous simulations run for various parameter combinations, we can draw the following conclusions. If the value j_2 is rather small, no value of j_1 provides a good match (we have considered various values of $\epsilon \leq 0.1$ for this purpose to understand the extent of the difference between the noise rules). This means that if the noise is induced only on a few nodes for the "0-1" rule, the two noise rules have different behavior regardless of how many nodes are perturbed with the "flip" rule. As j_2 increases, there are values of j_1 that yield a very good match of the two rules, as can be seen in Figure 4. We consider $N = 128, k = 8, \epsilon = 0.01, T = 50$, and values of $j_2 = 1, 2, \ldots, 120$. The probability $\mathcal{P}$ takes on many values in $(0, 1)$. We plot j_1 versus $\mathcal{P}$ and j_2. If no match is found then j_1 is set to -10 so we can identify more clearly the values of j_2 and $\mathcal{P}$ for which this happens. We observe that mostly small values of j_2 and large values of $\mathcal{P}$ generate a mismatch. Otherwise, there is generally an increasing trend for j_1 with increased values of j_2, and a decreasing trend of j_1 with increased values of $\mathcal{P}$. Further simulations reveal that larger connectivity k is associated with more matches as well as a flattening of the surface at a maximum level that decreases with increased k. In other words, if the connectivity is large, then there is a unique j_1 that is independent of $\mathcal{P}$ and j_2 for a large combination of these two parameters, that yields a good match of the two models. Also, the larger the k, the smaller the value of this unique j_1, and the wider the spread of the match. For the parameters mentioned above we observe a flattening of the surface for values of k around 32. On the other hand, small connectivity is associated with a sharper and higher peak in the surface and a clear dependance of j_1 on the values of both $\mathcal{P}$ and j_2 similar to what can be seen in Figure 4. We also note that for $\mathcal{P} = 0.5$ and ϵ very close to 0 the graph of j_1 versus j_2 yields a line with slope $1/2$ as expected.

We have run similar simulations with larger values of ϵ. The surfaces obtained cover a wider range of values for both $\mathcal{P}$ and j_2, which is to be expected. At the same time the values of j_1 tend to decrease with larger ϵ. However, it is desirable to consider small ϵ values since larger values could allow for situations in which some of the individual distances $|p_i(T) - q_i(T)|$ could be very small and others quite large, but still the condition $D \leq \epsilon\sqrt{I}$ would hold true.

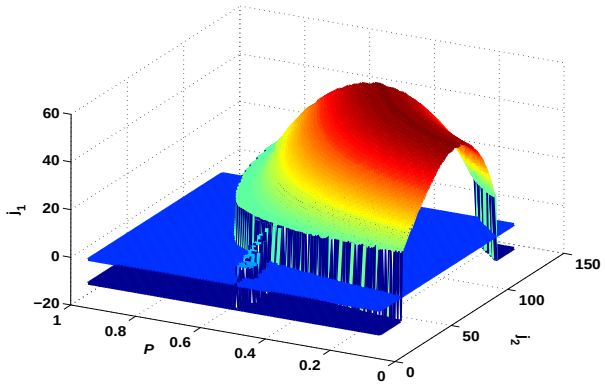

FIGURE 4. Plot of the results of the Euclidean distance procedure. We plot j_1 versus $\mathcal{P}$ and j_2 for the following parameters: $N = 128, k = 8, \epsilon = 0.01, T = 50, j_2 = 1, 2, \ldots, 120, \mathcal{P} \in (0, 1)$. If no match is found, then j_1 is set to -10. The plane through $j_1 = 0$ is graphed as well. We observe the dependence of j_1 on both $\mathcal{P}$ and j_2.

Given all of the above, we note that unless k and j_2 are sufficiently large, and $\mathcal{P}$ is sufficiently small, the two noise rules may yield different behavior. Also, for smaller values of k it is not possible to give a unique value of j_1 for each j_2 that would yield a match of the two noise rules. So, in what follows we will consider $\mathcal{P} \neq 1/2$ and compare the noise rules for $j_1 = j_2$ and smaller values of k, keeping in mind that in some cases there might be a larger value of j_1 that can make the two model behaviors equivalent. However, by doing this we are able to provide a comparison at the same level of noise in terms of number of perturbed nodes, and take into account the cases when the two noise rules cannot be matched. We are also able to understand the various dynamics that such noise rules can induce at various levels of the j values. Observe that due to the ranges of values for the functions $f(p)$ and $g(p)$, most differences between these two functions occur for small and especially large values of $\mathcal{P}$.

We start by generating consecutive iterations of the models (3) and (5) and plotting them on the same graph for an easy comparison. We perform simulations for a variety of combinations of the parameters j, k, and $\mathcal{P}$, but include only typical graphs in this paper. Note that the parameter k may have a significant impact on the long run behavior of the system.

In Figure 5 we plot the first, the second, and the 50-th iterations of the models (3) and (5) for values of $\mathcal{P}$ specified in each subplot. We graph the first diagonal as well, and all the plots are over the unit square. In all these figures $N = 128$, $k = 8$, and $j = 4$. We see that substantial differences occur for larger values of $\mathcal{P}$, while for small values the two models behave

somewhat the same. This is a feature that is noted for all the cases studied. Thus, the larger the $\mathcal{P}$, the more significant are the differences between the two models. The "flip" rule yields a less dynamic graph for the 50-th iteration, while the graph of the "0-1" rule generates more complexity. We observe that the number of fixed points of higher order iterates increases with $\mathcal{P}$, which is suggestive of a more dynamic behavior of the system. Further simulations show that an increase in k has the effect of flattening and elevating the curves towards 1. The behavior for large values of k is quite similar regardless of the actual value of k. Smaller values of k generate most of the qualitative differences between the models. However, in most cases, the values of $p(t)$ increase with increased k and therefore, for very large values of k the ranges for $p(t)$ can be very narrow and the two models produce very close graphs. This supports the previous findings regarding the flattening of the surface generated using the Euclidean distance for large values of k and a decrease of the values of j_1 with increased k. On the other hand, small values of the parameter j have most impact and generate more dynamic curves, while large values of j (not shown) make less of a qualitative difference in the behavior of the models in many cases and generate less complexity in the iterations. Last, all the comments above hold for other values of N (with a corresponding scaling of ranges of the parameters), and they support the previous findings in this section.

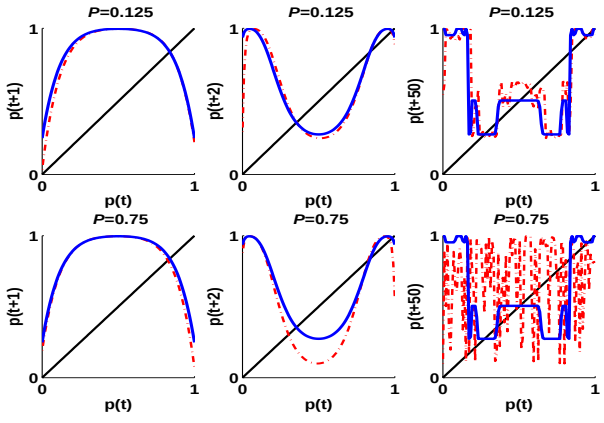

FIGURE 5. The first, second, and 50-th iterations of the noise models for a network with $N = 128$ nodes, and parameters $j = 4, k = 8, \mathcal{P} = 1/8$ and $7/8$ respectively. The "flip" rule is represented by a continuous curve, while the "0-1" rule by a dotted curve. The models generate a somewhat similar behavior for small $\mathcal{P}$, while for large values of $\mathcal{P}$ the "0-1" model generates more complexity.

We now turn to the comparison of the noise effects when the parameter j is random. We generate a new value of j at each time step according to a given distribution or random process. We use the following distributions: uniform on $\{1, 2, \ldots, N\}$, binomial with parameters N and θ, Poisson with parameter λ, and power law on $\{0, 1, \ldots, N\}$ and parameter γ. We study also the behavior under two stochastic processes: symmetric random walk starting at $0 < M < N$, and Poisson process with parameter $\lambda(t)$. In the simulations we vary the parameters of the random term j to identify what values induce differences in the overall behavior of the two noise rules.

We observe that the uniform distribution generates similar behaviors of the two models. The other distributions and processes induce differences mainly if the generated values of j are smaller and the values of $\mathcal{P}$ are larger. Thus, according to our observations, if the parameters of a distribution or random process are such that the generated values of j are small, then we can identify clear differences between the two noise rules. Also we note that a few large values of j can simplify the behavior of the models. Thus if one of the rules works mainly under smaller values of j while the other one generates also larger values of j, the differences are more clear.

In Figure 6 we show the case of the uniform distribution and $\mathcal{P} = 6/8, N = 128, k = 8$ in the first line, and two samples of a power law distribution with parameter $\gamma = 2$ in the second and third line. For each case we graph the first, the second, and the fiftieth iteration for both the "flip" rule and the "0-1" rule. We observe the simpler behavior in the case of the uniform distribution, and the more complex behavior induced by the power law. A situation similar to the power law distribution is observed for other distributions or random processes: binomial, Poisson, random walk, Poisson process. In Section 5 we will explore the impact of the magnitude of j on the behavior of the systems in more detail.

Now that we understand how the two noise rules work, we can proceed with the analysis of the robustness of the network to such disturbances. We will focus mainly on parameter values that have shown clear differences between the two noise models in the study above. Again, we keep in mind that in some instances there might be larger values of j for the "0-1" rule that could bring the two models to a similar behavior. We will see that there are situations in which in the long run the differences reduce, and other situations when the differences become very clear.

In the next section we provide a numerical analysis of the robustness through the study of bifurcation diagrams and Lyapunov exponent computations. Then we focus on an analytic

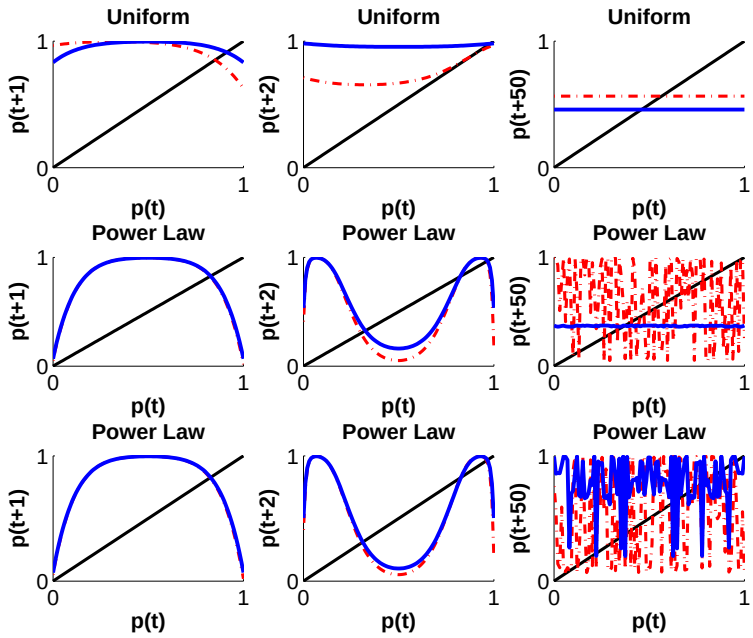

FIGURE 6. The first, second, and fiftieth iterations of the noise models ("flip" rule with continuous line, "0-1" rule with dotted line) for a network with $N = 128$ nodes, $k = 8$, and parameters j generated by a discrete uniform distribution on $\{1, 2, \ldots, N\}$, $\mathcal{P} = 6/8$ in the first line. The models generate a non-complex behavior despite the differences between them. The second and third lines correspond to two samples with values of j from a power law distribution with $\gamma = 2$. The models generate a more complex behavior and we can see the clear differences between them. A similar situation is observed for other distributions or random processes: binomial, Poisson, random walk, Poisson process. The differences are more clear for small j and large $\mathcal{P}$. Also, we note that large values of j induce less complex behavior of the graphs.

approach in which the models are simplified and some assumptions made for a more in depth view on iterations, bifurcations and fixed points.

4. Numerical Analysis of Robustness

We now turn toward a numerical analysis of the robustness of (3). Our methodology here is as follows. We iterate (1) enough times to pass through any transient stage. After this point, we use the perturbation schemes described in (3) and (5). That is to say, we keep track of two systems: the perturbed one, (3) or (5), and the unperturbed one, (1). In doing so, we seek to determine whether or not there exists any significant qualitative difference between the evolution of (1) and the evolution of (3) or (5).

For practical purposes, we separate the case of a fixed value of j and a random value of j throughout the computations.

In what follows we focus on bifurcation diagrams and Lyapunov exponents. We iterate the model a number of times to pass the transient phase and then we plot the resulting values of $p(t)$ for many initial conditions to create the bifurcation diagrams. In this way, we are able to better ascertain in what both k and j affect the long-term dynamics of both the unperturbed and perturbed systems. On the other hand, the so-called Lyapunov exponents, give us an indication as to the presence or absence of stability. To recall for the reader, the Lyapunov exponent is defined to be

$$L(x_0; f) = \lim_{n\to\infty} \left[\prod_{j=0}^{n-1} \left| f'(x_j) \right| \right]^{\frac{1}{n}},$$

where $f(x)$ is the map describing the evolution of the system from one time point to another, while $\{x_0, x_1, \ldots, x_n\}$ represents the trajectory of x_0 under the map f. When the Lyapunov exponent of an orbit is negative, the implication is that a stable orbit is attained. Conversely, when the Lyapunov exponent is positive, the implication is that chaos is present, provided that the orbit is not asymptotically periodic. For more on the Lyapunov exponent see [31] or [32].

The Lyapunov exponent calculation and the bifurcation diagrams indicate that both noise rules have a significant impact on the behavior of the system. The original system exhibits chaos through period doubling bifurcations as noted in [15] and [19]. This will be seen in Figure 7. We observe that the two types of perturbations induce order in the system which is more accentuated for larger values of j. More precisely, the range of values of k for which the system exhibits chaos is narrowed as j increases, until the system becomes completely ordered, with one period doubling bifurcation that could be reversed for larger values of j. The system exhibits only one stable fixed point for even larger values of j. The rate at which these changes take place is higher for the "flip" rule; that is the changes occur for smaller j values in this case. On the other hand, once the stable fixed point is reached, the "0-1" rule maintains it for all values of $j \leq N$ thereof. However, the "flip" rule reverses the process due to the symmetry of the rule with respect to the number of ones and zeros in the system, so that for very large j there is another transition back to chaos.

The differences between the effects of the two perturbations are even more clear for large values of $\mathcal{P}$ as noted in the previous section, but the overall behavior is similar.

In Figure 7 we show the Lyapunov exponents and corresponding bifurcation diagram for the original system (1) that has been iterated 500 time points prior to plotting to surpass the transient stage. The initial value for the Lyapunov exponent is set to 0.3 in all the figures, but other values yield similar behavior. We note that it may happen that for some parameter values the Lyapunov exponent of the orbit of 0.3 is not defined, the orbit containing points that yield a null derivative of the model. Also, observe that if the system reaches $p(t) = 0$, then $p(t+1) = 0$ too. In other words, 0 is a fixed point for the original system. Then, the Lyapunov exponent is $\ln(k+1) > 0$.

In Figure 8 the first column corresponds to Lyapunov exponents and corresponding bifurcation diagram for the "flip" rule with $j = 1$, while the second column represents similar plots for the "0-1" rule. We observe the differences between the rules, as well as the difference between the noise induced systems and the original system presented in Figure 7. Periodic windows are clearly observed in the case of the "0-1" rule. We note that for both rules larger values of j have the effect of narrowing the range of values corresponding to chaos. For large j values the system exhibits order with one period doubling bifurcation that can be reversed with increased connectivity k. We note that the flip rule exhibits symmetry in terms of values of j. For example, for $j = 127$ the bifurcation diagram for the "flip" rule is identical to that for $j = 1$, while the one for the "0-1" rule shows only stable fixed points.

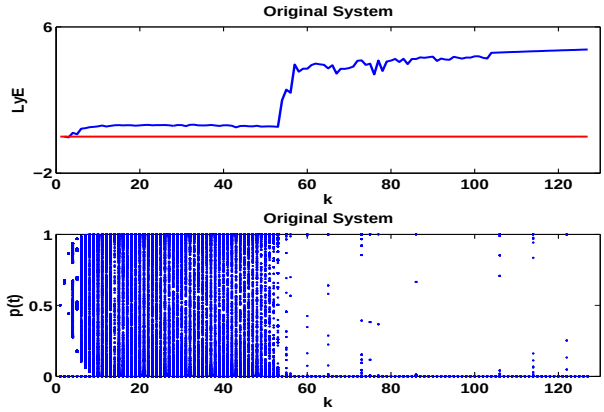

FIGURE 7. Lyapunov Exponents (LyE) and bifurcation diagram for the original system (1) with $N = 128$.

We focus now on noise rules driven by a random j. We observe again that differences between the two noise rules occur only for small values of j and moderate or large values of $\mathcal{P}$, or cases when one rule works mainly under smaller values of j, while for the other rule there are at least

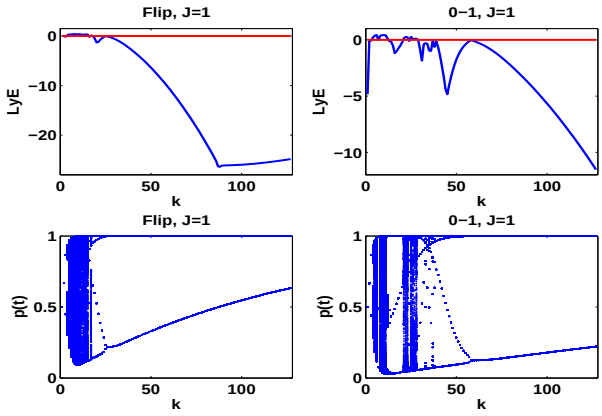

FIGURE 8. Lyapunov Exponents (LyE) and bifurcation diagram for the perturbed system with $N = 128, \mathcal{P} = 3/4$, and $j = 1$. The first column represents the "flip" rule, and the second column represents the "0-1" rule. We can see differences in the two noise rules. We note that for both rules larger values of j have the effect of narrowing the range of values corresponding to chaos. For large j values the system exhibits order with one period doubling bifurcation that can be reversed with increased connectivity k.

occasional large values of j. Since the differences are more clear for large $\mathcal{P}$, in the following simulations we set $\mathcal{P} = 3/4$.

In Figure 9 we consider the two noise rules driven by a power law distribution with parameter $\gamma = 2.5$. The "flip" rule is represented in the first column and the "0-1" rule in the second column. We observe that the system is mostly ordered, although the bifurcation diagrams show a nontrivial behavior. We note that in general the systems exhibit chaos only for small values of k. For small values of γ the bifurcation diagrams tend to "fan out" indicating higher order periodicity paired with negative Lyapunov Exponents. The "fanning" covers a wider range of values of $p(t)$ for the "0-1" rule. As γ increases the "fanning" is replaced by lower order periodicity, and the graphs resemble the ones in Figure 8.

We note here that for the case of a uniform distribution on $\{0, 1, 2, \ldots, N\}$ and a Poisson distribution with small parameter λ the results resemble the "fanning" behavior of the power law distribution. However the ranges of k corresponding to chaos are generally wider than in the case of the power law distribution. For a Poisson distribution with large parameter λ the graphs resemble the ones for the binomial distribution in Figure 10. The case of a Poisson process with parameter λ yielding values of j close to the ones used for the Poisson random variable generates similar results.

In Figures 10, 11 we present similar plots for the binomial distribution and the random walk with the specified parameters. In each figure we can see that the noise generally induces order, although this can be done differently depending on the underlying noise rule and random variable

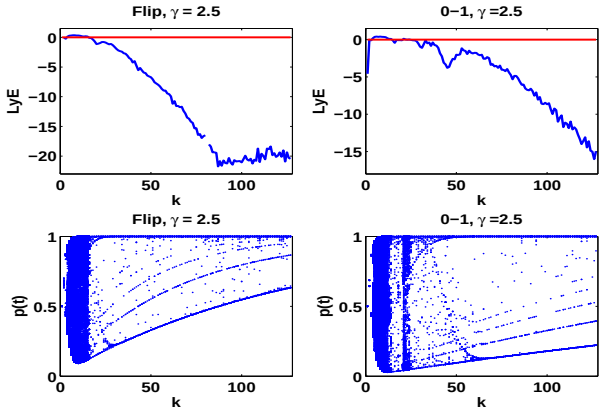

FIGURE 9. Lyapunov Exponents (LyE) and bifurcation diagram for the perturbed system with $N = 128, \mathcal{P} = 3/4$, and values of j from a power law distribution on $0, 1, \ldots, N$ with parameter $\gamma = 2.5$. The first column represents the "flip" rule, and the second column represents the "0-1" rule. The noise induces order in the system for larger k values for both types of perturbations, with some differences in the two noise rules. The bifurcation diagrams show a nontrivial behavior.

j. If the parameters are such that the values of j are rather large, the system exhibits lower order periodicity. We also note that in some cases the bifurcation diagrams "fan out" indicating an ordered, but nontrivial behavior. They correspond to negative Lyapunov exponents. This is more clear in the case of larger $\mathcal{P}$ and smaller j values. All the sample graphs presented in this paper are representative for the behavior observed.

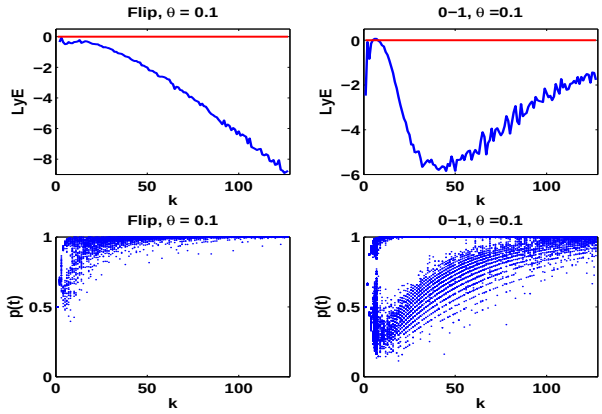

FIGURE 10. Lyapunov Exponents (LyE) and bifurcation diagram for the perturbed system with $N = 128, \mathcal{P} = 3/4$, and values of j from a binomial distribution with parameters N and $\theta = 0.1$. The first column represents the "flip" rule, and the second column represents the "0-1" rule. We can see that the noise induces order in the system, with some differences in the two noise rules. The "flip" rule generates a symmetric behavior with respect to the values of θ; e.g. the graphs are the same for $\theta = 0.9$. In general, for both rules larger values of j are associated with lower order periodicity.

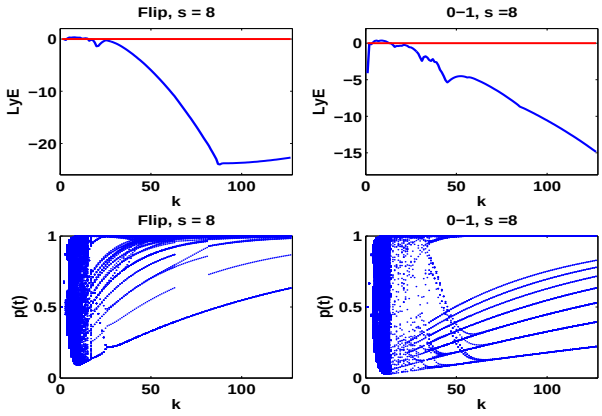

FIGURE 11. Lyapunov Exponents (LyE) and bifurcation diagram for the perturbed system with $N = 128, \mathcal{P} = 3/4$, and values of j from a symmetric random walk starting at $s = 8$. The first column represents the "flip" rule, and the second column represents the "0-1" rule. We can see that the noise induces order in the system, with some differences in the two noise rules.

Finally, we note that it is observed that for small values of k 3-cycles may occur both in the perturbed system and the unperturbed system, and this, of course, would suggest by Sharkovskii's Theorem that cycles of all orders exist for these systems [31].

Now, in addition to varying k while holding the other parameters fixed, we also varied N for various choices of k and the other parameters held fixed at the values previously mentioned. However, it did not appear that variation in N had any interesting or noteworthy affect on the qualitative behavior of either the perturbed or unperturbed system, therefore we do not provide any figures associated with these changes.

5. Focus on Iterations, Fixed Points, Bifurcations, and Delay Plots

In this section, we wish to examine analytically the noise induced models (3) and (5). In particular, we are interested in how the function $p(t)$ behaves under repeated iterations in the case when it is perturbed. That is to say, we will examine how (3) and (5) behave when we iterate them repeatedly. Now, to facilitate this exploration, we shall change slightly the formulation of our model. In particular, the functions that we examine in this section are

$$f(p) = 1 - (p + \alpha(1-2p))^{k+1} - (1 - p - \alpha(1-2p))^{k+1}, \tag{6}$$

and

$$g(p) = 1 - (p + \alpha(\mathcal{P}-p))^{k+1} - (1 - p - \alpha(\mathcal{P}-p))^{k+1}. \tag{7}$$

where α is a parameter that indicates the proportion of nodes that are perturbed – that is, changed – at each iteration. We make the note here that the notation in this section should not be confused with the similar notation used in Section 3. In particular, in the noise models (3) and (5) we have $\alpha = \frac{j}{N}$. Thus, since according to previous observations, the size of j is important in the behavior of the system, we simplify the two models by considering the proportion of changed nodes instead of the exact number of changed nodes. Note that if j is random, α can be viewed as the average number of changed nodes divided by N.

What we will see is precisely that which has been described previously in this paper – namely, that for very small and very large α the perturbed "flip" system behaves chaotically for small connectivity, whereas for α between these extremes, the behavior of the perturbed system is quite ordered. Succinctly, some noise can attenuate the chaos of the original system, but too much noise has the opposite effect. The "0-1" system exhibits chaos for a wider range of connectivity values, and the perturbed system becomes ordered at a slower rate with increased α.

First we will take a look again at the iterations of the two systems (6) and (7) by condensing in three dimensional graphs an entire range of k values for a fixed α value. Figure 12 presents plots of $f^i(p)$ versus p and k, with $i = 1, 4$ and 50 respectively in the first row. The second row contains similar plots for $g^i(p)$ versus p and k. Here $k = 1, 2, \ldots 20$, $\mathcal{P} = 3/4$, and $\alpha = 0.05$ meaning that 5% of the nodes are perturbed by noise. We note the effect of k on the shape of the graphs showing a complex behavior for small k and less complex graphs for larger k values. The graphs for the "0-1" rule $g(p)$ tend to be more complex overall. We also observe that higher order iterates induce complexity in the system for small α, while an increase in α generates simpler graphs which produce an ordered behavior. This trend is slower for the "0-1" rule. This supports the previous discussions on the impact of the values j on the behavior of the system.

Now let us analyze the fixed points of the two maps. According to the noise iterations seen in Section 3, we should be able to analyze them numerically with the help of Matlab. First observe that the fixed point conditions, namely $f(p) = p$ and $g(p) = p$ in the equations (6) and (7), can be written as follows:

$$1 - p = (p + \alpha(1 - 2p))^{k+1} + (1 - p - \alpha(1 - 2p))^{k+1} \tag{8}$$

and

$$1 - p = (p + \alpha(\mathcal{P} - p))^{k+1} + (1 - p - \alpha(\mathcal{P} - p))^{k+1} \tag{9}$$

respectively.

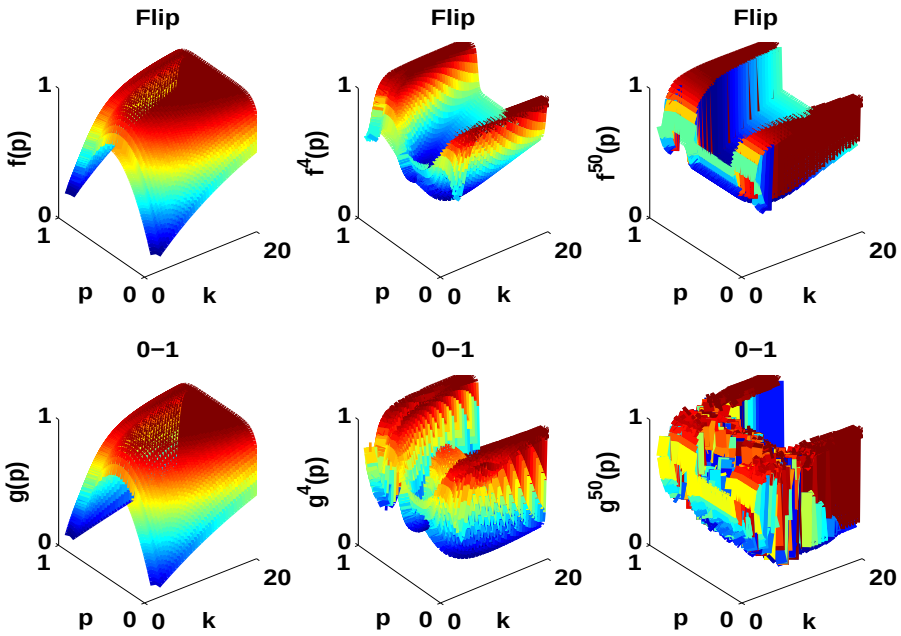

FIGURE 12. Plots of iterations $f^i(p)$ versus p and k, with $i = 1, 4$ and 50 respectively in the first row. The second row contains similar plots for $g^i(p)$ versus p and k. Here $k = 1, 2, \ldots 20$, $\mathcal{P} = 3/4$, and $\alpha = 0.05$ meaning that 5% of the nodes are perturbed by noise. We note that larger k induces less complexity in the long run behavior. At the same time $g(p)$ generates more complex graphs than $f(p)$. We also observe in simulations (not shown) that larger α induces simpler graphs which correspond to fewer fixed points.

In both cases it is clear that if $k \to \infty$ then $p \to 1$. Although $p = 0$ is a fixed point for the original system, it is not for the noise induced systems.

We use Matlab to solve numerically the two equations for various values of k and α. We graph the results for the original system and the two noise induced systems on the same graph for comparison. In Figure 13 we present plots corresponding to $\alpha = 0.2$ only for simplicity. The fixed points are computed for $k = 1, 2, \ldots, 20$. We can see that the fixed points approach indeed 1 as k increases, and we notice that the two noise rules generate different fixed points. The values of the fixed points are closer for small or large values of α. At the same time, we can see that the fixed points of the "0-1" rule overlap with the original system for the small selected α and small k values. At the same time we note that large α generates an overlap of the fixed points of the original system with the "flip" rule. The rate of convergence to 1 appears to be higher for medium values of α.

We are interested now in identifying ranges of parameters for which the fixed points are stable. To this aim we first look at the function $f\prime(p)$ where p is a fixed point of the map (6). Later we will do the same for the map (7). We would like to see for what values of the fixed

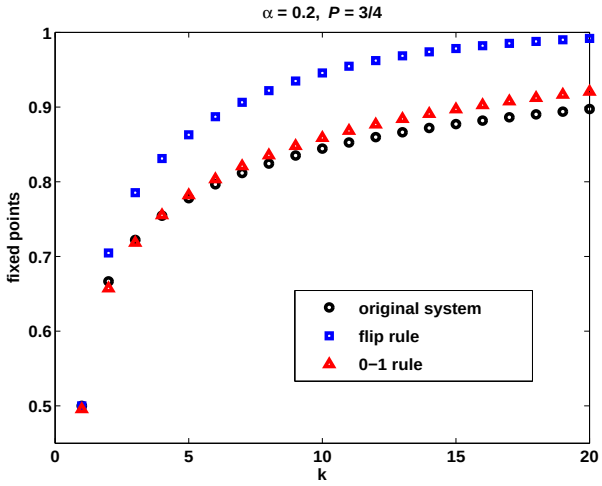

FIGURE 13. Fixed points for the original system, the "flip" rule, and "0-1" rule for $\alpha = 0.2$ and for $\mathcal{P} = 3/4$. The fixed points approach 1 but at different rates in all three cases.

point p the derivative takes on values less than (or greater than) 1 in absolute value, since it is known [31] that for a smooth map $f(p)$ and a fixed point p, $|f\prime(p)| < 1$ implies that p is stable, and $|f\prime(p)| > 1$ implies that p is unstable.

Observe that the derivative of the map (6) can be written as

$$f\prime(p) = (k+1)(1-2\alpha)\left[(1-p-\alpha(1-2p))^k - (p+\alpha(1-2p))^k\right] \tag{10}$$

while the fixed point condition (8) can be rewritten as

$$(1-p-\alpha(1-2p))^k = \frac{1-p-(p+\alpha(1-2p))^{k+1}}{1-p-\alpha(1-2p)}. \tag{11}$$

Clearly, equation (11) can be solved only numerically with the help of the computer. To understand what values of p satisfying the fixed point condition (11) yield a value of (10) less than 1 in absolute value, we replace (11) into the expression of $f\prime(p)$ to get

$$f\prime(p) = (k+1)(1-2\alpha)\frac{1-p-(p+\alpha(1-2p))^k}{1-p-\alpha(1-2p)}. \tag{12}$$

Then we use Matlab to plot this function for various values of α and k. The result is in Figure 14. In each subplot we graph the function (12) for $k = 1, 2, 8, 10$ for simplicity, while α varies as specified in each plot. We observe that medium values of α yield wider ranges of values of p for which $|f\prime(p)| < 1$. For example, if $\alpha = 0.4$ the graphs for $k = 1$ is completely contained in the horizontal strip between the lines $y = -1$ and $y = 1$, so any fixed point is stable. As k increases the graphs concentrate towards the right side of the subplots. For $k = 10$ the range of values of p that yield stability is the most narrow. This is suggestive of the fact that for larger α higher

order fixed points may develop as observed in the previous sections. Taking into account that according to Figure 13 the fixed points have mainly values larger than 0.5, we can see that in many cases they could exhibit stability as seen in the corresponding subplots of Figure 14. Also, if $\alpha = 0.5$ all the fixed points are stable since the derivative is null.

In a similar fashion we can deal with the "0-1" rule. The derivative $g\prime(p)$ in which the fixed point condition is replaced can be written as

$$g\prime(p) = (k+1)(1-\alpha)\frac{1-p-(p+\alpha(\mathcal{P}-p))^k}{1-p-\alpha(\mathcal{P}-p)}. \tag{13}$$

We observe that the graphs (not shown) are similar to those for the "flip" rule with small α and there is a reduced range of values of p yielding stability. The overall tendency of the graphs for various values of k is to slowly bend to the left as α increases so that the plots for $\alpha = 0.9$ in the "0-1" model is similar to the plots for $\alpha = 0.4$ in the "flip" model. At the same time we observe that there is no "reverse" behavior of the "0-1" rule as it is the case with the "flip" rule.

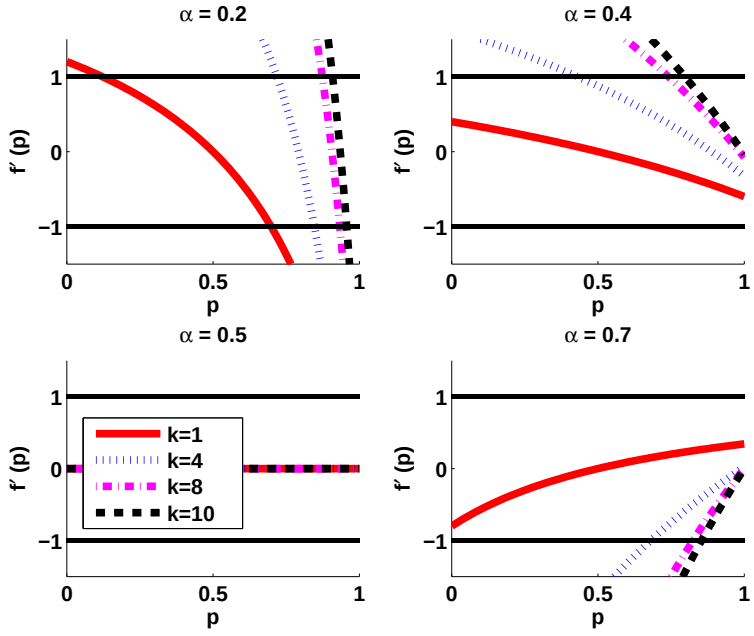

FIGURE 14. The graph of $f\prime(p) = (k+1)(1-2\alpha)\frac{1-p-(p+\alpha(1-2p))^k}{1-p-\alpha(1-2p)}$. Here α is varied as specified in each subplot. Each graph represents the superimposed plots for $k = 1, 4, 8, 10$. We observe that as k increases the graphs tend to concentrate towards the right side of each subplot, and the ranges of values of p yielding stability is narrowed. Medium values of α generate the widest ranges of stability in terms of values of the fixed points, while $\alpha = 0.5$ yields only stable fixed points. By comparing this figure with Figure 13 we can deduce that in many cases the fixed points could yield stability.

This enforces the previously observed differences between the rules: in general, the "0-1" rule generates a more complex behavior for a wider range of parameter values than the "flip" rule,

which is in agreement with the more narrow ranges for stability. Higher order fixed points are expected.

We note here that the observations regarding the stability of the fixed points are in agreement also with the fact that the fixed points converge to 1 as k increases. Also, the original system yields a graph similar to the one for $\alpha = 0.2$ in Figure 14.

We complete the analysis above by generating bifurcation diagrams for the models (6) and (7) regarding the two functions as functions of both α and k. We generate bifurcation diagrams both along α and along k for a deeper analysis of the phenomenon. In Figure 15 the first line corresponds to the "flip" rule. The upper left corner represents bifurcation diagrams along k for several fixed values of α, while the upper right corner represents bifurcation diagrams along α for several fixed values of k. The second line represents the corresponding diagrams for the "0-1" rule. We observe that the diagrams along k are in agreement with previous bifurcation diagrams presented in Section 4. More complex behavior occurs for small values of α. As α increases, the chaos is replaced by one period doubling bifurcation which then turns into a stable fixed point. Observe that the ranges of α are different in the diagrams along k. For values larger than the ones for the "flip" rule along k, the system exhibits stable fixed points as for $\alpha = 0.15$ shown in the graph, and for $\alpha > 1/2$ the diagrams are reversed by the symmetry exhibited by this rule. On the other hand, in the case of the "0-1" rule along k the symmetry does not occur. Regarding the diagrams along α, we can identify the symmetric behavior for the "flip" rule and that the initial complex behavior for very small α is transformed into a period doubling bifurcation for larger values of α and one stable fixed point for medium values of α. As k increases the system has fixed points of order one or two. The "0-1" rule exhibits a somewhat similar overall behavior without the symmetry and with clearly different ranges of the parameters.

In summary for the "flip" rule, in the case where the proportion of nodes changed at each step is quite small or quite large, the behavior of the perturbed system is disordered and chaotic. Conversely, in the case where the proportion of nodes changed at each step is between these extremes, the behavior of the system is ordered, and the chaos is suppressed. The "0-1" rule yields a more complex behavior, but again displays disorder and chaos for small α and order for medium or large α. In either case, a large connectivity is associated with order in the system. Thus, this analysis does not reveal a unique critical noise value α that can make the separation between order and chaos for all underlying parameters.

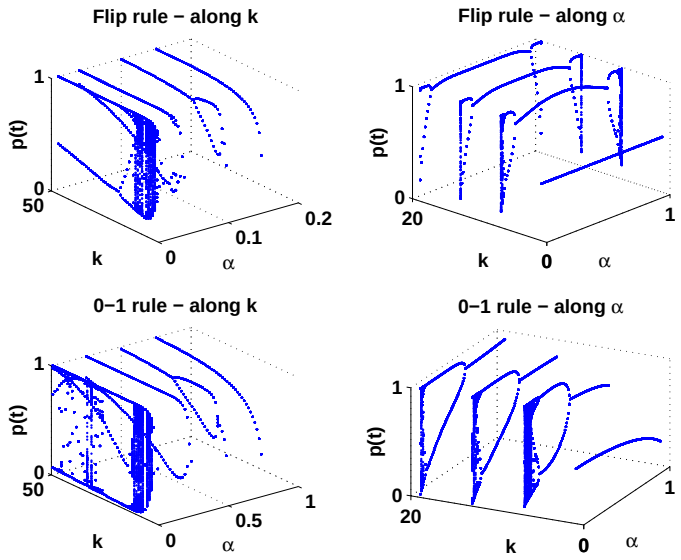

FIGURE 15. Bifurcation diagrams for the models (6) and (7). The first line represents the "flip" rule with diagrams along k and α as specified, while the second line represents the corresponding graphs for the "0-1" rule. We can observe that these diagrams are in agreement with previous observations in Section 4.

We also note that the use of α simplifies the view of the models and cannot capture all the complex behavior exhibited by the case when j is random as seen in Section 4.

We end this analysis with a look at delay plots for a more clear view of the attractors of the system. We plot $p(t+1)$ versus $p(t)$ and $p(t-1)$ for a set of 100 consecutive time points, and for several values of k and a fixed value of α. The system is iterated 1000 times prior to plotting to surpass the transient period. In Figures 16, 17, 18 we do this for the original system (1), the "flip" rule (6), and the "0-1" rule (7) respectively. In all these figures $\alpha = 0.01$. The values of k are specified in the subplots and they are the same for all three figures for a direct comparison.

The shades produced by a coloring procedure indicate if there are ordered (same color in a determined area) or chaotic attractors (the colors do not follow any pattern). For example, in Figure 16, we observe ordered attractors of period one for $k = 1$, period two for $k = 3$, and period five for $k = 5$. On the other hand, for $k = 10$ for example, there is no ordering of the shades and this is suggesting that the points change in an irregular, chaotic fashion. We observe that the ranges of k for order versus chaos are supporting the information provided by Figure 7. Similarly, we observe the ranges of ordered and chaotic attractors for the two noise rules in the other two figures, and we note the agreement with previous observations, and the difference between the noise procedures. For other values of α the attractors agree with the

previous observations that more order is induced in the system, but with differences between the two noise rules.

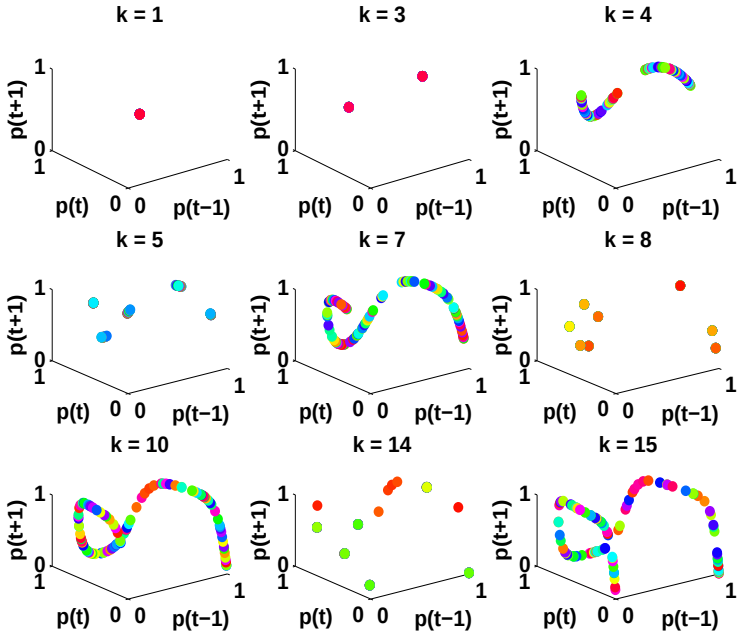

FIGURE 16. Three-dimensional delay plot ($p(t+1)$ versus $p(t)$ and $p(t-1)$) for a series of 100 consecutive time points generated with the original system (1). Here $\alpha = 0.01$ and the values of k are as specified in each graph. The shades induced by a coloring procedure suggest ordered attractors for some values of k, such as $k = 1, 3, 5$ and chaotic attractors for values such as $k = 10$. This agrees with the bifurcation diagram of Figure 7.

6. Conclusions

In this paper, we have explored both analytically and numerically the models (3) and (5). These models compute the probability, p, that a given node is in the ON state provided that each node has k parents and that, after some fixed period of time has elapsed, at each successive time step, j nodes are changed according to the schemes previously described – i.e., (3) and (5). We have seen that the introduction of noise into the system affects markedly the dynamics of the system. In particular, we have seen that while (1) exhibits chaotic behavior for a rather wide range of k values, (3) and (5) behave very differently. Specifically, as $j \to N$ we find that, at first, the region of chaotic behavior is compressed. For larger j the chaotic region disappears altogether and the behavior of the system is ordered.

Thus, we conclude that the introduction of noise into this particular system actually has a stabilizing effect on the dynamics of the system. Indeed, by introducing enough noise, the system

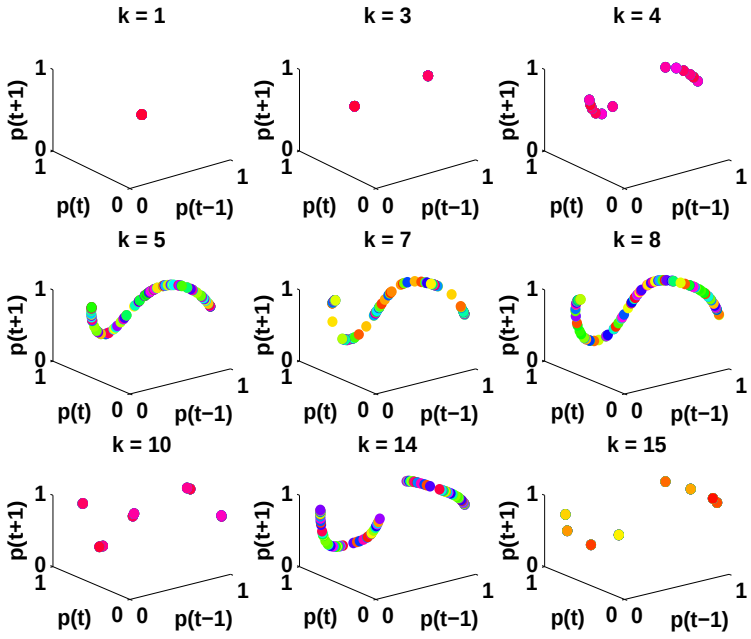

FIGURE 17. Three-dimensional delay plot ($p(t+1)$ versus $p(t)$ and $p(t-1)$) for a series of 100 consecutive time points generated with the "flip" rule (6). The parameters have the same values as in Figure 16. We observe again the ordered and chaotic attractors for ranges of k that agree with previous observations.

is made to behave in an ordered way for a wide range of values of k, the number of parents. Now, it would seem, on intuitive grounds at least, that as the number of nodes changed per step is increased, chaos might be reintroduced into the perturbed system. Put another way, it would seem that by changing too many nodes per step, the increasingly many perturbations would actually destabilize the system. And, in fact, this is precisely what happened for the "flip" rule, due to its symmetric behavior. Indeed, by changing too many nodes per iteration, we saw that the perturbed system could be destabilized if k is small enough. On the other hand, due to its definition and behavior, the "0-1" rule does induce order regardless of the amount of noise introduced. Overall, large values of k are associated with an ordered behavior.

There exist myriad other avenues for future study. For instance, it would be interesting to see how robust the system is to other perturbation schemes that correspond to say genetic mutations or neural network activities. For example, adding or removing connections or nodes dynamically in the system would mimic genetic mutations. It would be of interest to parametrize the noise by assigning a probability that each node flips its value, or it is assigned a random value with a given probability as it is done in [29] and [30]. On the other hand, given the intrinsic connection between Boolean networks and neural networks, it would be of interest to induce the noise according to a threshold rule that would take into account the weighted sum of the parent

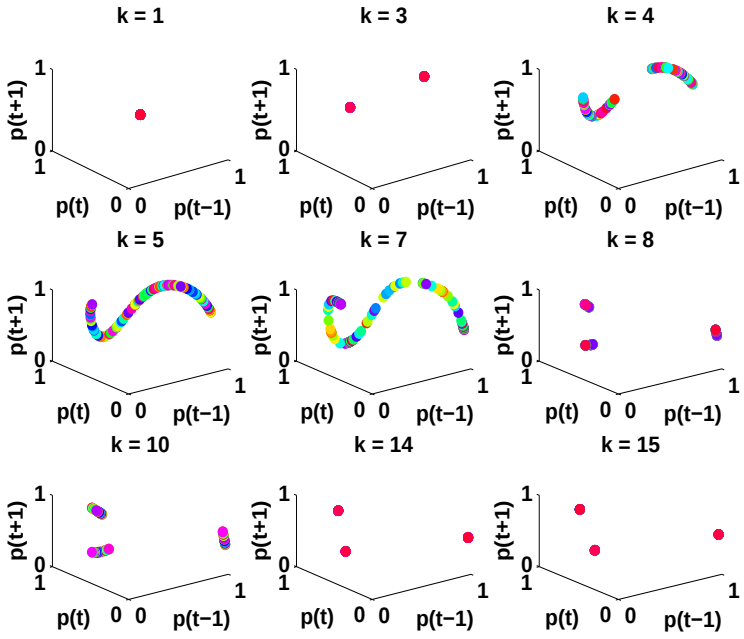

FIGURE 18. Three-dimensional delay plot ($p(t+1)$ versus $p(t)$ and $p(t-1)$) for a series of 100 consecutive time points generated with the "0-1" rule (7). The parameters have the same values as in Figure 16. We observe again the ordered and chaotic attractors for ranges of k that agree with previous observations. Also, we note the differences between the two noise rules.

values for each node. The dynamical organization in the presence of noise of a Boolean neural network with random connections has been analyzed by Huepe and Aldana in [9], showing that there exists a critical value of a noise parameter used by the authors that separates order from random behavior. A similar study would be of interest in the context of this paper.

Moreover, it might well be of interest to examine the robustness of networks whose nodes do not update at the same time and are, therefore, asynchronous. Various types of asynchronous random Boolean networks have been studied with specific updating schemes and Boolean rules ([4], [11], [13] - [15], [33] - [36]). The asynchrony itself generates a certain level of noise in the system. However, inducing other types of noise can complement the asynchrony and account for more than one type of disturbance that can impact the behavior of the system.

Applying a similar analysis for the case when the number of parents vary from one node to another and expanding the analysis to other Boolean rules is a future goal. For example, extending the analysis to Probabilistic Boolean Networks introduced by Shmulevich et. al. [37] as models for gene-regulatory networks and studied extensively during the last years [38] - [41], would allow us to use more than one Boolean rule for each node according to a random selection procedure, and therefore mimic the dynamical behavior of genetic networks. On the

other hand, considering a power-law distribution for the number of parents would supplement previous findings regarding the robustness of scale-free networks [1].

At the same time, taking into account the topology of the network, as opposed to randomly selecting the parent nodes is another possibility. It is known that the variation of topology of the network from random to, say, regular or scale-free network has a clear impact on pattern formation in binary cellular automata as observed by Marr and Hütt [17], [42]. Embedding the topology in the network model could lead to interesting results regarding the effect of topology variation on the robustness to perturbations.

Succinctly, there are many possibilities for additional study of these models and their behavior under various perturbations.

References

[1] M. Aldana and P. Cluzel, *A Natural Class of Robust Networks*, PNAS, 100, 15, p. 8710-8714, 2003.

[2] Andrecut M., Ali M. K., *Chaos in a simple Boolean network*, International Journal of Modern Physics B, Vol. 15, 1 (2001), p. 17-23.

[3] M. Chaves, R. Albert, E.D. Sontag, *Robustness and fragility of Boolean models for genetic regulatory networks*, J. Theoretical Biology 235, p. 431-449, 2005.

[4] Cornforth D., Green D.G., Newth D., Kirley M., *Do artificial ants march in step? Ordered asynchronous processes and modularity in biological systems* , Artificial Life VIII, MIT Press, 2002, p. 28-32.

[5] Fox J.J., Hill C.C., *From topology to dynamics in biochemical networks*, Chaos, Vol. 11, 4 (2001), p. 809-815.

[6] Greil F., Drossel B., *The dynamics of critical Kauffman networks under asynchronous stochastic update*, Phys. Rev. Lett. 95, 048701, 2005.

[7] Heidel J., Maloney J., Farrow C., Rogers J.A., *Finding cycles in synchronous Boolean networks with applications to biochemical systems*, International Journal of Bifurcation and Chaos, 13 (2003), p. 535-552.

[8] Huang S., *Genomics, complexity and drug discovery: insights from Boolean network models of cellular regulation*, Pharmacogenomics, 2, 3 (2001), p. 203-222.

[9] Huepe C., Aldana-González M., *Dynamical Phase Transition in a Neural Network Model with Noise: An Exact Solution*, Journal of Statistical Physics, 108, Nos. 3/4, 2002.

[10] Kauffman S.A., Peterson C., Samuelsson B., and Troein C., *Genetic networks with canalyzing Boolean rules are always stable*, PNAS, Vol. 101 (49), p. 17102-17107, 2004.

[11] Low S., Lapsley D., *Optimization flow control, i: Basic algorithm and convergence*, IEEE/ACM Transactions on Networking, 1999.

[12] Matache M.T., Heidel J., *A Random Boolean Network Model Exhibiting Deterministic Chaos*, Physical Review E, 69, 056214, 2004.

[13] Matache M.T., Heidel J., *Asynchronous Random Boolean Network Model Based on Elementary Cellular Automata Rule 126*, Physical Review E, 71, 026232, 2005.

[14] Matache M.T., *Asynchronous Random Boolean Network Model with Variable Number of Parents based on Elementary Cellular Automata Rule 126*, IJMPB, Vol. 20, 8, p. 897-923, 2006.

[15] Deng X., Geng H., Matache M.T., *Dynamics of Asynchronous Random Boolean Networks with Asynchrony Generated by Stochastic Processes*, Biosystems, in press.

[16] Wolfram S., *A new kind of science*, Wolfram Media, Champaign, 2002.

[17] Marr C., Hütt M.-T., *Similar impact of topological and dynamic noise on complex patterns*, Physics Letters A, 349, p. 302-305, 2006.

[18] Kauffman S.A., *The origins of order*, Oxford University Press, 1993, p. 173-235.

[19] Andrecut M., *Mean field dynamics of random Boolean networks*, J. Stat. Mech., P02003 (2005).

[20] S. Bilke and F. Sjunnesson, *Stability of the Kauffman Model*, Physical Review, E 65, 016129, 2001.

[21] M. Chaves, E.D. Sontag, R. Albert, *Methods of robustness analysis for Boolean models of gene control networks*, IEE Proc. Systems Biology, to appear.

[22] N. A. Fatès, M. Morvan, *An experimental study of robustness to asynchronism for elementary cellular automata*, Complex Systems , Vol. 16 (1), pp. 1-27, 2005.

[23] I. Schmulevich and S. A. Kauffman, *Activities and Sensitivities in Boolean Network Models*, Physical Review Letters, 93, 4, 2004.

[24] I. Schmulevich, H. Lähdesmäki, E. Dougherty, J. Astola, and W. Zhang, *The Role of Certain Post Classes in Boolean Network Models of Genetic Networks*, PNAS, 100, 19, 2003.

[25] Gershenson C., Kauffman S.A., and Shmulevich I., *The Role of Redundancy in the Robustness of Random Boolean Networks*, in Rocha, L. M., L. S. Yaeger, M. A. Bedau, D. Floreano, R. L. Goldstone, and A. Vespignani (Eds.), Artificial Life X, Proceedings of the Tenth International Conference on the Simulation and Synthesis of Living Systems, MIT Press, p. 35-42, 2006.

[26] J. Fan, X. Li, X.F. Wang, *On synchronous preference of complex dynamical networks*, Physica A, 355, p. 657-666, 2005.

[27] A.L. Barabási, R. Albert, H. Jeong, *Mean-field theory for scale-free random networks*, Physica A, 272, p. 173-187, 1999.

[28] J. Fan, X.F. Wang, *On synchronization in scale-free dynamical networks*, Physica A, 349, p. 443-451, 2005.

[29] Moreira A.A., Mathur A., Diermeier D., Amaral L.A.N., *Efficient system-wide coordination in noisy environments*, PNAS, 101, 33, p. 12085-12090, 2004.

[30] Amaral L.A.N., Diaz-Guilera A., Moreira A.A., Goldberger A.L., Lipsitz L.A., *Emergence of complex dynamics in a simple model of signaling networks*, PNAS, 101, 44, p. 15551-15555, 2004.

[31] Alligood K.T., Sauer T.D., Yorke J.A., *Chaos: An Introduction to Dynamical Systems*, Springer-Verlag, 1996.

[32] R. C. Robinson, *An Introduction to Dynamical Systems*, Prentice Hall, 2004.

[33] Gershenson C., *Classification of Random Boolean Networks*, Artificial Life VIII, Standish, Abbass, Bedau (eds) (MIT Press), 2002, p. 1-8.

[34] Harvey I., Bossomaier T., *Time out of joint: attactors in asynchronous random Boolean networks*, Proceedings of the Fourth European Conference on Artificial Life (ECAL97), MIT Press, 1997, p. 65-75.

[35] Kanada Y., *The effects of randomness in asynchronous 1D cellular automata*, Proceedings of ALIFE IV, 1994.

[36] Thomas R., ed., *Kinetic Logic: A Boolean approach to the analysis of complex regulatory systems*, Lecture Notes in Biomathematics, Springer Verlag, 29 (1979).

[37] I. Shmulevich, E. R. Dougherty, S. Kim, W. Zhang, *Probabilistic Boolean Networks: A Rule-based Uncertainty Model for Gene Regulatory Networks*, Bioinformatics, Vol. 18, No. 2, pp. 261-274, 2002.

[38] M. Brun, E. R. Dougherty, I. Shmulevich, *Steady-State Probabilities for Attractors in Probabilistic Boolean Networks*, Signal Processing, Vol. 85, No. 4, pp. 1993-2013, 2005.

[39] E. R. Dougherty and I. Shmulevich, *Mappings Between Probabilistic Boolean Networks*, Signal Processing, Vol. 83, No. 4, pp. 799-809, 2003.

[40] H. Lähdesmäki, S. Hautaniemi, I. Shmulevich, O. Yli-Harja, *Relationships Between Probabilistic Boolean Networks and Dynamic Bayesian Networks as Models of Gene Regulatory Networks*, Signal Processing, Vol. 86, No. 4, pp. 814-834, 2006.

[41] I. Shmulevich, E. R. Dougherty, W. Zhang, *Gene Perturbation and Intervention in Probabilistic Boolean Networks*, Bioinformatics, Vol. 18, No. 10, pp. 1319-1331, 2002.

[42] Marr C., Hütt M.-T., *Topology regulates pattern formation capacity of binary cellular automata on graphs*, Physica A, 354, p. 641-662, 2005.